Temporal and spatial variations of CO2, CH4 and N2O fluxes at three differently managed grasslands

Author(s):
Imer, Dennis; Merbold, Lutz; Eugster, Werner; Buchmann, Nina

Publication date:
2013-02-14

Permanent link:
https://doi.org/10.3929/ethz-b-000077873

Originally published in:
Biogeosciences Discussions 10, https://doi.org/10.5194/bgd-10-2635-2013

Biogeosciences Discuss., 10, 2635–2673, 2013
www.biogeosciences-discuss.net/10/2635/2013/
doi:10.5194/bgd-10-2635-2013

Biogeosciences Discussions
Open Access

Temporal and spatial variations of CO_2, CH_4 and N_2O fluxes at three differently managed grasslands

D. Imer, L. Merbold, W. Eugster, and N. Buchmann

Grassland Sciences Group, Institute of Agricultural Sciences, ETH Zurich, Zurich, Switzerland

Received: 26 January 2013 – Accepted: 4 February 2013 – Published: 14 February 2013

Correspondence to: D. Imer (dimer@ethz.ch)

Published by Copernicus Publications on behalf of the European Geosciences Union.

Abstract

A profound understanding of temporal and spatial variabilities of CO_2, CH_4 and N_2O fluxes between terrestrial ecosystems and the atmosphere is needed to reliably quantify these fluxes and to develop future mitigation strategies. For managed grassland ecosystems, temporal and spatial variabilities of these three greenhouse gas (GHG) fluxes are due to environmental drivers as well as to fertilizer applications, grazing and cutting events. To assess how these affect GHG fluxes at Swiss grassland sites, we studied three sites along an altitudinal gradient that corresponds to a management gradient: from 400 m a.s.l. (intensively managed) to 1000 m a.s.l. (moderately intensive managed) to 2000 m a.s.l. (extensively managed). Temporal and spatial variabilities of GHG fluxes were quantified along small-scale transects of 16 static soil chambers at each site. We then established functional relationships between drivers and the observed fluxes on diel and annual time scales. Furthermore, spatial variabilities and their effect on representative site-specific mean chamber GHG fluxes were assessed using geostatistical semivariogram approaches. All three grasslands were N_2O sources, with mean annual fluxes ranging from 0.15 to 1.28 nmol m^{-2} s^{-1}. Contrastingly, all sites were net CH_4 sinks, with uptake rates ranging from −0.56 to −0.15 nmol m^{-2} s^{-1}. Mean annual respiration losses of CO_2, as measured with opaque chambers, ranged from 5.2 to 6.5 µmol m^{-2} s^{-1}. While the environmental drivers and their respective explanatory power for N_2O emissions differed considerably among the three grasslands (adjusted r^2 ranging from 0.19 to 0.42), CH_4 and CO_2 fluxes were much better constrained (adjusted r^2 ranging from 0.41 to 0.83), in particular by soil water content and air temperature, respectively. Throughout the year, spatial heterogeneity was particularly high for N_2O and CH_4 fluxes. We found permanent hot spots for N_2O emissions and CH_4 uptake at the extensively managed site. Including these hot spots in calculating the mean chamber flux was essential to obtain a representative mean flux for this ecosystem. At the intensively managed grassland, management effects clearly dominated over effects

BGD
10, 2635–2673, 2013

of environmental drivers on N_2O fluxes. For CO_2 and CH_4, the importance of management effects did depend on the status of the vegetation.

1 Introduction

About 10 % of the fossil fuel emissions that originate from EU-25 countries can be absorbed by terrestrial ecosystems (Janssens et al., 2003; Schulze et al., 2009). While most of the atmospheric CO_2 is sequestered by forests, grasslands are a small net sink for atmospheric CO_2. Croplands are reported to be CO_2 neutral, and managed peatlands act as net sources for atmospheric CO_2 (Ciais et al., 2010b). However, the net terrestrial sink for atmospheric CO_2 is almost counterbalanced by CH_4 and N_2O emissions from agriculture (Ciais et al., 2010a). Despite the relatively small atmospheric concentrations of CH_4 and N_2O, these two greenhouse gases (GHG) account for 26 % of the global warming effect due to their high global warming potential (GWP) on a per mass basis over a 100 year time horizon (IPCC, 2007). Thus, understanding temporal and spatial variabilities of CO_2, CH_4 and N_2O fluxes between terrestrial ecosystems and the atmosphere is of key importance to reliably estimate these fluxes and to develop mitigation strategies. While Vleeshouwers and Verhagen (2002) and Janssens et al. (2003) reported that the GWP of European grasslands is still highly uncertain, Soussana et al. (2007) and Schulze et al. (2009) estimated that European grasslands had negative GWPs. In particular, all investigated grasslands were net sinks for CO_2 on an annual time scale. The fluxes of CH_4 and N_2O, expressed in CO_2-equivalents, reduced the net CO_2 sink effect, but were too small to change the overall effect into a positive GWP. Theses two studies, however, did not consider altitudinal variations. Because mountains under episodic influences of maritime air masses receive additional orographic precipitation as compared to lowland sites (Beniston, 2005), soils may be more likely to emit CH_4 and N_2O under such conditions.

Many studies use manually-operated closed soil chambers to measure fluxes of CO_2, CH_4, and N_2O (Flessa et al., 2002; Pumpanen et al., 2004; Wang et al., 2005;

BGD
10, 2635–2673, 2013

Jones et al., 2006; Jiang et al., 2010; Rochette, 2011), as they are applicable in a wide range of ecosystems with varying site conditions. Moreover, chamber methods, in contrast to the eddy covariance method, are capable of detecting small flux magnitudes which are characteristic for CH_4 and N_2O fluxes (Baldocchi et al., 2012). In addition, the use of chambers allows to detect spatial patterns in GHG fluxes (Flessa et al., 2002; Merbold et al., 2011), an important aspect when studying managed or undulating grassland sites (Ambus and Christensen, 1994; Ball et al., 1997; Mathieu et al., 2006). Especially N_2O and CH_4 fluxes are known for their non-uniform spatial distribution of sources and sinks (e.g. Matthias et al., 1980; Folorunso and Rolston, 1984; van den Pol-van Dasselaar et al., 1998). The spatial patterns are often controlled by vegetation and soil properties such as soil type and texture, soil temperature and soil water content as well as soil C and N contents and microtopography (e.g. Dalal and Allen, 2008). In managed grasslands, temporal variability of GHG fluxes needs to be taken into consideration as well, because flux magnitudes respond not only to environmental forcings but also to human induced activities such as grazing, cutting and fertilization (Buchmann, 2011).

To understand how annual GHG balances respond to environmental and management induced forcings, we quantified temporal and spatial variations of chamber-based CO_2, CH_4 and N_2O fluxes of three Swiss grasslands, which are part of a traditional three stage farming system at different altitudes (Weiss, 1941; Boesch, 1951; Ehlers and Kreutzmann, 2000). Our specific objectives were: (1) to investigate the source/sink behavior of CO_2, CH_4 and N_2O fluxes at three differently managed grasslands; (2) to assess temporal variation of GHG fluxes at diel, seasonal and annual time scales; and (3) to identify the relevance of spatial variations of GHG fluxes for annual budget calculations.

BGD
10, 2635–2673, 2013

2 Materials and methods

2.1 Site description

The three stage farming system that is typical for many parts of the Swiss Alps (Ehlers and Kreutzmann, 2000) was represented exemplarily by the three ETH research sites Chamau (CHA), Fruebuel (FRU) and Alp Weissenstein (AWS). The lowland site is represented by CHA, situated north of Lake Zug in the pre-alpine lowlands of Switzerland at 400 m a.s.l. (47°12′37″ N, 8°24′38″ E), with an annual mean temperature of 9.1 °C and 1151 mm of precipitation (Sieber et al., 2011; Finger et al., 2012). The pastures typically represent the winter location for sheep and cattle and are used for forage production. Our site is intensively managed, with five to ten management events per calendar year, which include cutting and/or fertilizer application. The exact number of management events per calendar year naturally depends on seasonal weather conditions and thus biomass growth.

The so-called Maiensaess site (early season mountain rangeland) is represented by FRU, situated at the Zugerberg mountain ridge, east of Lake Zug (47°6′57″ N, 8°32′16″ E) at 1000 m a.s.l., with an annual mean temperature of 6.1 °C and 1682 mm of precipitation (Sieber et al., 2011; Finger et al., 2012). The pastures at FRU are used for cattle grazing in late spring (May) and early fall (September). The management includes two to four cuts and/or fertilization events per calendar year, again depending on local weather conditions and resulting vegetation growth.

The alpine site is represented by AWS, situated near the Albula pass at 2000 m a.s.l. in the Grisons (46°34′59″ N, 9°47′25″ E), with an annual mean temperature of −1.4 °C and 877 mm of precipitation (Sieber et al., 2011; Finger et al., 2012; Michna et al., 2013). AWS represents the summer rangelands for cattle grazing where grass is not cut in normal years. However, manure is applied to pastures at the end of the grazing season, typically in the second half of September.

BGD
10, 2635–2673, 2013

The geographic location of the three sites as well as the site setups are shown in Fig. 1. For a detailed description of species composition of the three grasslands, see Zeeman et al. (2010).

2.2 Experimental setup

From June 2010 to June 2011, we measured fluxes of CO_2, CH_4 and N_2O using opaque static soil chambers at the three sites CHA, FRU and AWS. The diameter of the polyvinyl chloride chambers was 0.3 m and the average head-space height 0.136 m (±0.015 m) (Hartmann et al., 2011). Chamber lids were equipped with reflective aluminum foil to minimize heating inside the chamber during the period of actual measurement. At each site, transects of 16 soil chamber collars were set up in May 2010 (Fig. 1). Spacing between the chambers was 7 m at CHA and FRU, and 5 m at AWS. At FRU, two transects were established, one consisting of 12 chambers and a second consisting of four chambers (Fig. 1c). This was done to adopt the sampling approach to the usual cutting regime, which is coerced by field parcels. Spacing was chosen so that the transects would fit into the previously calculated footprint of the eddy covariance towers at the respective sites (Zeeman et al., 2010). The collars were not moved over the 12 months of study to avoid effects of soil disturbance and to maintain their spatial distribution. Sampling of the chambers was performed on a weekly basis during the growing season, and at least once a month during the winter season (except for AWS which is inaccessible in winter). The vegetation inside the chamber collars was manually cut at the times of regular management activities, i.e. cuts and grazing.

Additionally, we measured diel patterns of CH_4 and N_2O fluxes in an intensive observation campaign in September 2010. During this campaign, CH_4 and N_2O fluxes were measured over 48 consecutive hours at all three sites simultaneously, at intervals of two hours.

BGD
10, 2635–2673, 2013

2.3 Data acquisition and processing

2.3.1 Flux sampling and calculations

GHG fluxes were calculated based on the rate of changing gas concentrations inside the chamber head space. After closing the chambers, four samples were taken, one immediately after closure and then at 10 to 13 min increments, so that the chamber was closed no longer than 40 min. A deployment time < 40 min is considered short enough to neglect saturation effects inside the head space and to avoid temporal changes of flux drivers (Scott et al., 1999). We used 60 mL syringes inserted into the chambers' lid septums to take the gas samples, then injected the gas into pre-evacuated 12 mL vials (Labco Limited, Buckinghamshire, UK). Prior to the second, third and fourth sampling of each chamber, the chamber head space was flushed with the syringe volume of air from the chamber head space to minimize effects of built up concentration gradients inside the chamber. Gas samples were analyzed for their CO_2, CH_4 and N_2O concentrations using gas chromatography (Agilent 6890 gas chromatograph equipped with a flame ionization detector and an electron capture detector, Agilent Technologies Inc., Santa Clara, USA) as described by Hartmann et al. (2011).

Data processing, which included flux calculation and quality checks, was carried out with the R statistical software (R Development Core Team, 2010). The rate of change was calculated by the slope of the linear regression between gas concentration and time. Fluxes were always small enough that no curvature in measured concentration data could be detected which would be indicative for saturation effects inside the chamber. We used the following equation to derive the flux estimate F_{GHG}:

$$F_{GHG} = \frac{\delta c}{\delta t} \cdot \frac{p \cdot V}{R \cdot T \cdot A} \quad (1)$$

where c is the respective GHG concentration (µmol for CO_2; nmol for CH_4 and N_2O). Time (t) is given in seconds, atmospheric pressure (p) in Pa, the head space volume (V) in m^3, the universal gas constant (R) is 8.3145 m^3 Pa K^{-1} mol^{-1}, T is ambient air

BGD
10, 2635–2673, 2013

temperature (K), and A is the surface area enclosed by the chamber (m^2). Individual chamber fluxes were only computed if the linear regression yielded a $r^2 \geq 0.8$. Consequently, we obtained CO_2, CH_4 and N_2O fluxes per chamber which were then filtered for obvious out of range values (±10 SD) for each sampling campaign. Chambers for which the rate of change of CO_2 was negative were also discarded, as photosynthesis is assumed to be zero inside the opaque chamber. The mean chamber flux was then calculated as the arithmetic mean of all available individual chamber fluxes at a site.

On the annual time scale, a total of 81 sampling campaigns were performed at the three sites in the period from June 2010 to June 2011 ($N_{CHA} = 35$; $N_{FRU} = 32$; $N_{AWS} = 17$), resulting in an equivalent number of mean chamber fluxes of N_2O, CH_4 and CO_2. We follow the micrometeorological convention, where positive fluxes are directed to the atmosphere and negative fluxes to the ecosystem. During the 48 h intensive observation campaign at all three sites (21–23 September in 2010), 75 mean chamber fluxes of CH_4 and N_2O were obtained at the three sites ($N_{CHA} = 25$; $N_{FRU} = 25$; $N_{AWS} = 25$).

2.3.2 Ancillary measurements

At each site, the following environmental variables were recorded as 10 minute averages: air temperature (T_a) at 2 m (HydroClip S3, Rotronic AG, Basserdorf, CH), soil temperature (T_s) at −0.02 m (TL107 sensors, Markasub AG, Olten, CH), volumetric soil water content (SWC) at −0.05 m (ML2x, Delta-T Devices Ltd., Cambridge, UK), and photosynthetic active radiation (PAR) at 2 m (PARlite, Kipp and Zonen B.V., Delft, The Netherlands). The position of these measurements is indicated by the star in Fig. 1. Leaf area index (LAI) of the vegetation outside the chambers was measured at each flux sampling campaign (LAI-2000, Licor, Lincoln, USA), i.e. every week during the growing period and at least monthly during winter (when there was no snow cover). LAI measurements thus represent averages of 12 measurements along the chamber

BGD
10, 2635–2673, 2013

transects. For regression modeling, we calculated temporal means of each variable in accordance to the length of flux sampling during each campaign.

2.3.3 Statistics

For each site, mean chamber GHG fluxes were used to establish functional relationships with environmental drivers, on diel and annual time scales, using simple linear regression models for diel and stepwise multiple linear regression models for annual time scales. A standardized principle component analysis (PCA) was performed prior to multiple linear regressions to minimize potential artifacts from co-linearities between environmental drivers. For the multiple linear regression models, the relative importance of each driver within the regression model was estimated using hierarchical partitioning (Chevan and Sutherland, 1991). The uncertainty of the calculated relative importance was assessed using parametric bootstrapping methods (Efron, 1979).

To investigate spatial variability of GHG fluxes, first a one-way analysis of variance (ANOVA) was used. The chamber number along the transect (Fig. 1) was used as predictor and all valid annual flux values per chamber were used. To assess the statistical significance of pairwise comparisons of ANOVA results, the Tukey honest significant differences (HSD) test was used. Then, empirical variograms on the basis of arithmetic mean fluxes per chamber were inspected for the 12-month study period and for distinct climatic seasons. If a significant difference of GHG fluxes among the 16 chambers was confirmed by ANOVA, Tukey HSD and by visual inspection of the empirical variograms, ordinary kriging was used to model the impact on spatial flux patterns (Ribeiro and Diggle, 2001). We tested four different estimation approaches to derive modeled semivariograms of spatial variation of GHG fluxes: (1) maximum likelihood (ML), (2) restricted maximum likelihood (RML), (3) ordinary least squares (OLS), and (4) weighted least squares (WLS) methods (Dietrich and Osborne, 1991). While least squares fitting generally works best with normally distributed data, maximum likelihood methods tend to be better suited for non-normally distributed ensembles. Thus, leave-one-out cross-validation was performed to assess model performance (Stone, 1974). Sill, range and

BGD
10, 2635–2673, 2013

nugget values were initialized based on visual inspection of the empirical variograms. Data were extrapolated for the length of the transect using a 1 m × 1 m grid.

3 Results

3.1 Temporal variation of GHG fluxes

3.1.1 Annual flux patterns and management

In general, fluxes of N_2O and CO_2 showed the expected seasonality, with highest emission rates during the summer months (Fig. 2). Contrastingly, CH_4 fluxes did not follow any seasonal trend.

At all three sites, N_2O fluxes were mostly positive, indicating a source for atmospheric N_2O. Occasional uptake was observed for mean and individual chamber fluxes, as indicated by the 95 % confidence interval in Fig. 2. Highest N_2O efflux rates were observed at CHA (intensively managed) shortly after fertilizer applications. These peak fluxes exceeded maximum N_2O fluxes at FRU (moderately managed) and AWS (extensively managed) by a factor of two and higher. At AWS, peak emissions were not only in correspondence with fertilizer application but also with grazing. The first peak period observed at AWS in 2010 coincided with the alpine grazing period, which spans from 15 June to 15 September. The mean N_2O efflux over the 12-month study period was highest at CHA with 1.28 nmol m^{-2} s^{-1} and lowest at FRU with 0.15 nmol m^{-2} s^{-1}. At AWS, an average efflux of 0.23 nmol m^{-2} s^{-1} was observed.

At CHA and FRU, both positive and negative CH_4 fluxes were observed, yet uptake dominated at both sites. During eight sampling campaigns, which represented 20 % of all campaigns, CHA was a source of CH_4. FRU was a source during five sampling campaigns, representing 12.5 % of all campaigns, while AWS acted as a sink for atmospheric CH_4 throughout the measurement period. Yet, no measurements are available for the winter period at this site. The response of CH_4 fluxes to fertilizer application was

BGD
10, 2635–2673, 2013

not as distinct as for N_2O fluxes. Over the 12-month study period, mean uptake rates for CH_4 were −0.15, −0.22 and −0.56 nmol m^{-2} s^{-1} at CHA, FRU and AWS, respectively.

Temporal flux patterns of CO_2 were comparable at all three sites. The annual range of flux magnitudes was slightly smaller at AWS than at CHA and FRU. Respiration increased after fertilizer application at all three sites, yet the magnitude of response was variable (Fig. 2). Over the 12-month study period, mean respiration rates were comparable at CHA and FRU, with 6.5 and 6.3 µmol m^{-2} s^{-1}, respectively. At AWS, respiration rates were slightly smaller, with an overall mean flux of 5.2 µmol m^{-2} s^{-1} (only during growing season).

3.1.2 Response of annual fluxes to environmental drivers

A PCA was performed to select an appropriate set of driver variables for the multiple linear models (Fig. 3) to investigate the underlying mechanistic processes that drive the small-scale GHG flux variability. With this PCA, we were able to identify similarities among potential driver variables (T_a, T_s, SWC, PAR, and LAI) and to reduce the set of driver variables for exploring functional relationships to those drivers that (a) are as independent from each other as possible, and (b) which are of similar relevance at all three elevations, such that functional relationships built with the selected drivers can be compared among sites. At CHA and FRU, T_a and T_s had similar loadings (Fig. 3) because both followed a similar annual cycle. Since T_a generally had the higher explanatory power than T_s, we selected T_a for our model. The first and second principal components further indicated that PAR and SWC may be treated as one variable at CHA and FRU (Fig. 3), where variations in PAR were of opposite sign compared to variations in SWC, simply indicating that episodic increases in SWC after rain events at the lower two sites coincided with periods of high cloudiness that reduced PAR over several days. In contrast, under fair weather conditions, the typical diurnal cycle of PAR was linked to a similar cycle of SWC in the opposite direction where (surface) soils got drier during the day and were replenished via capillary rise and maybe hydraulic redistribution in the vascular plant root systems at night. Since our selection of T_a already

BGD
10, 2635–2673, 2013

represented atmospheric conditions at a site, we selected SWC instead of PAR as the second variable. The third variable selected via PCA was LAI which was almost independent of SWC at all three sites (Fig. 3) and hence was expected to add explanatory value to a functional model where the three compartments atmosphere (T_a), soil (SWC) and vegetation (LAI) were represented (Fig. 4).

The explanatory power of the multiple linear model with regard to the temporal variation of N_2O fluxes varied considerably at the three sites, with adjusted r^2 values ranging from 0.19 to 0.42 (Table 1). The relative importance (RI) of each selected driver, i.e. the contribution to the overall variance of flux variability explained by the model, was not consistent among sites (Fig. 4). At CHA, the model was able to explain 42 % of the total variance inherent in annual N_2O flux data, with LAI and T_a being the most important explanatory variables (RI_{LAI} = 45 %; RI_{Ta} = 38.9 %). SWC had much less influence on the N_2O efflux, with a RI of 16.1 %. At FRU, T_a was clearly the most important driver, with a RI of 84.7 %, followed by SWC with a RI of 14 %. LAI was of minor importance, with a RI of 1.3 %. In total, only 19 % of the variance in N_2O fluxes was explained by the model at FRU. At AWS, 34 % of the variance were explained. Here, SWC was the most powerful explanatory variable, with a RI of 54.7 %, followed by LAI (RI = 43.7 %). T_a had almost no impact on the variability of the N_2O flux at AWS (RI = 1.7 %).

The variation of explanatory power among the driver variables within the multiple linear model for the prediction of CH_4 fluxes was even more pronounced than that for N_2O fluxes (Table 1). Yet, CH_4 fluxes were better constrained by the set of drivers, with adjusted r^2 values ranging from 0.41 to 0.83. Again, the RI of the drivers was not consistent among sites (Fig. 4). At CHA, the model explained 41 % of the total variance inherent in all annual CH_4 flux data, with LAI and SWC being the most influential variables (RI_{LAI} = 40.7 %; RI_{SWC} = 38.8 %), followed by T_a with a RI of 20.4 %. At FRU, 51 % of the total variance was explained, with SWC being the most important variable, exhibiting a RI of 84 %. At AWS, 83 % of variance was explained by the model, of which 82.7 % were due to changes in SWC. At both sites, FRU and AWS, the variables LAI and T_a had minor influences on CH_4 fluxes.

BGD
10, 2635–2673, 2013

The explanatory power of the multiple linear model for CO_2 fluxes was almost the same at CHA and FRU, with 80 % total explained variance (Table 1). At AWS, the model was still able to explain 47 %. At CHA and FRU, T_a clearly was the most influential variable with RI values of 71 and 81 %, respectively. Yet, at least at CHA, LAI had a considerable influence on the temporal variability of CO_2 fluxes, with a RI of 21.8 %. At FRU, the contribution of seasonal changes in LAI was considerably less important (RI = 9.1 %). At AWS, T_a was the most important variable in the model similar to CHA and FRU (RI of 55.7 %), followed by SWC with a RI of 30.9 % (Fig. 4).

3.1.3 Diel variation of N_2O and CH_4 fluxes

Mean chamber efflux rates of N_2O and mean chamber uptake of CH_4 were observed during the intensive observation campaign at all sites in September 2010 (Fig. 5). The diel N_2O flux magnitudes along the elevational transect yielded a different ranking among sites than that observed at the annual scale. During the intensive observation campaign, highest emissions of N_2O were measured at AWS, with an average flux of 0.54 nmol m^{-2} s^{-1}, followed by CHA with 0.21 and FRU with 0.15 nmol m^{-2} s^{-1}. Diel variations of N_2O fluxes were clearly found only at FRU, where high emission rates were observed during the day and smaller emissions during nights (Fig. 5), as expected from bacterial activity that follows the diel cycle of temperature. T_a was a good predictor for N_2O efflux rates at the diel time scale at CHA and FRU, explaining 54 and 59 % of the variance, respectively. In contrast, N_2O emissions did not significantly correlate with T_a at the diel scale (nor at the annual scale) at AWS (Fig. 4).

Highest mean uptake rates of CH_4 were measured at AWS with −0.47 nmol m^{-2} s^{-1}, followed by CHA and FRU with −0.31 and −0.16 nmol m^{-2} s^{-1}, respectively (Fig. 5). Although considerable variation in CH_4 flux rates was visible at CHA and FRU, no obvious diel trend was identified. At AWS, CH_4 uptake rates were almost constant with only very little temporal variation. Hence, regression analysis to determine flux drivers was not successful. At CHA, 13 % of the variance in CH_4 uptake rates could

BGD
10, 2635–2673, 2013

be explained by T_a, while no significant relationship could be established at FRU and AWS. SWC variations, important at the annual scale, were not large enough during the 48 hour intensive observation campaign to develop any explanatory power at the diel scale.

3.2 Spatial variation of GHG fluxes

3.2.1 Spatial heterogeneity of GHG fluxes on diel scale

Spatial heterogeneity in N_2O fluxes was largest at AWS, followed by FRU and CHA, as indicated by the 95 % confidence interval in Fig. 5, probably due to large variations in SWC. While spatial heterogeneity was small and almost constant over the season at CHA, it increased with increasing N_2O efflux rates at FRU and AWS. In this context it is worth noting that AWS received a manure application 10 days prior to the intensive observation campaign, as this is common practice shortly before the end of the alpine grazing season.

Except for one chamber, spatial heterogeneity of CH_4 fluxes measured at FRU was comparable at FRU and AWS, least heterogeneity was observed at CHA. In contrast to increasing spatial heterogeneity in N_2O fluxes with higher efflux rates, spatial variability of CH_4 fluxes seemed to be quite constant over time at all three sites.

3.2.2 Spatially invariant hot spots of GHG fluxes on annual scale

Spatial variability of annual average N_2O fluxes, i.e., the flux variation among chambers along the transect, was highest at CHA (Fig. 6), much in contrast to the spatial variation seen over 48 hours. The one-way ANOVA with chamber as factor yielded a p-value of 0.57 for N_2O fluxes, indicating that all chambers showed high variation during the 12 months of measurements. At AWS, chambers one to three showed a wider range of annual average N_2O efflux rates relative to the other chambers along the transect. Yet, due to some very high flux estimates, the ANOVA yielded a p-value of 0.52, indicating

BGD
10, 2635–2673, 2013

no significant differences among individual chambers. This suggested that the spatial variability of N_2O fluxes was not larger than the temporal variability of the fluxes measured at AWS. Spatial variations of annual average N_2O fluxes at FRU were negligible (Fig. 6), and in a similar magnitude as at the diel scale (Fig. 5).

Spatially rather homogeneous annual average CH_4 fluxes were found at CHA and FRU (Fig. 6), similar to the small spatial variation at the diel scale (Fig. 5). At AWS, we observed a spatially invariant spot of significantly ($p = 0.02$) lower CH_4 uptakes rates around chambers two and three (Fig. 6).

3.2.3 Spatial auto-correlation of GHG fluxes

The key to a representative statistical ensemble of GHG flux averages for each site (here reported as mean chamber fluxes) is that measurements of individual chambers are varying randomly, independent of their adjacent chambers. If this statistical assumption is not met, then spatial auto-correlation may introduce a bias in site flux averages. For none of the three GHGs, such auto-correlations were found at CHA and FRU, as confirmed by geostatistical semivariogram analysis. At CHA, spatial auto-correlation of N_2O fluxes was only observed for short periods (7 days) directly after fertilization events (data not shown).

In contrast to these findings, all three annual average GHG fluxes per chamber showed considerable spatial auto-correlation at AWS (Fig. 7). Hence, we assessed the potential bias that this spatial auto-correlation might introduce in GHG flux estimates for this site using the geostatistical semivariance approach.

For annual average fluxes of N_2O per chamber, the semivariance steadily increased up to a spatial separation of 40 m, where it seemed to reach its local sill value at 0.057 nmol m^{-2} s^{-1}, suggesting auto-correlation of N_2O fluxes along the transect at AWS (Fig. 7). After the range value of 40 m, the semivariance dropped to a level of approximately 0.025 nmol m^{-2} s^{-1} and fluctuated around it. For annual average fluxes of CH_4 per chamber, semivariance (Fig. 7) also steadily increased, but did not reach a sill value at the maximum observed lag (80 m), which was the length of the transect. The

BGD
10, 2635–2673, 2013

maximum range of semivariance of CH_4 fluxes was 0.039 nmol m^{-2} s^{-1}. Contrastingly, the semivariance of annual average fluxes of CO_2 per chamber seemed to be rather constant over space at lags between 20 and 60 m, before the semivariance increased rapidly up to 1.81 µmol m^{-2} s^{-1} (Fig. 7). This did indicate that the three GHG fluxes at AWS responded to different processes acting at different spatial scales.

To assess the influence of the observed spatial auto-correlation on spatially modeled CH_4 and N_2O, but also on CO_2 fluxes, we used four fitting approaches to compute empirical variograms; maximum likelihood (ML), restricted maximum likelihood (RML), ordinary least squares (OLS) and weighted least squares fitting (WLS). These four fitting methods were inspected for their performance using leave-one-out cross validation. The best performing model in terms of agreement between observation and model was subsequently employed for ordinary kriging to spatially interpolate fluxes along the transect (Table 1).

Visually we found that least squares and maximum likelihood techniques generally yielded differently shaped fits (Fig. 7). For N_2O and CH_4 fluxes, likelihood methods were best suited, with better agreement between observations and the model than least squares fits (Table 1). This was expected as N_2O and CH_4 flux data are not normally distributed. For CO_2 fluxes, however, model selection had only a small effect. Yet, overall performance was best, as indicated by highest r^2 values, for the ordinary linear regression (Table 1).

4 Discussion

It was not a priori expected that the three grasslands at different elevations and thus management intensities were all net sinks for methane due to abundant precipitation in mountainous areas, whereas the tight coupling between N_2O efflux rates and fertilizer applications confirmed earlier studies. However, important differences between annual and diel time scales were found. In addition, N_2O as well as CH_4 fluxes were highly

BGD
10, 2635–2673, 2013

variable in time and space, supporting previous studies (e.g. Folorunso and Rolston, 1984; Mosier et al., 1991; Velthof et al., 2000).

4.1 Annual GHG fluxes and drivers of their temporal variability

4.1.1 N_2O fluxes

Our measurements give strong evidence that managed grasslands are a constant source of N_2O, as hardly any uptake was observed (Ryden, 1981; Wagner-Riddle et al., 1997; Glatzel and Stahr, 2001; Neftel et al., 2007). The small number of negative N_2O fluxes (uptake) observed was evenly distributed throughout the 12-month study period. As expected, the intensively managed site, CHA, was the strongest source of N_2O. While total N addition at CHA was on average three times higher (per application) compared to FRU, mean annual emissions were more than eight times those at FRU. The latter site was characterized by the lowest mean annual N_2O emissions.

Our findings also underline the challenge of predicting N_2O fluxes from grasslands. N_2O fluxes were weakly constrained by a set of three environmental variables. Their influence on the flux varied temporally and from site to site, indicating the importance of additional factors (e.g. land management, fertilizer application). Yet, our results are in agreement with previous studies, which identified air temperature and soil water content as influential variables (e.g. Wang et al., 2005; Liebig et al., 2010; Schaufler et al., 2010). The high relative importance of LAI at CHA (intensively managed) can be explained by the fact that step-changes in LAI due to regular cuts during the growing season reflect subsequent fertilizer applications at CHA (N addition usually within five days after the cut). This finding underlines the importance of a realistic management consideration when predicting N_2O fluxes. This was corroborated in Fig. 8, which shows the response of the three GHG fluxes to their primary environmental driver (at two LAI classes) on the annual scale (Table 2). For N_2O we found that T_a had no significant influence on flux magnitudes if LAI was kept constant. Thus, management (with LAI as proxy) had a larger effect on N_2O fluxes than the envronment (with T_a as proxy).

BGD
10, 2635–2673, 2013

4.1.2 CH_4 fluxes

Our results showed consistently small CH_4 sinks at all three sites, well in agreement with other studies on temperate grasslands in the lowlands (Mosier et al., 1997; Liebig et al., 2010). Positive CH_4 fluxes mostly occurred during periods with high SWC and/or after manure application (Lessard et al., 1997), and hence were observed most frequently at the intensively and moderately intensive managed site, CHA and FRU. For FRU, our results are not fully in agreement with Hartmann et al. (2011), who exclusively measured uptake of CH_4 at FRU in the years 2007, 2008 and 2009. However, their measurements were taken at generally drier soils, supporting the idea of regulating effects of SWC on CH_4 fluxes (RI of 84 %). At the extensively managed AWS site, both, Hartmann et al. (2011) and this study exclusively observed uptake of CH_4.

Annually, CH_4 fluxes were well predictable, being mostly constrained by SWC (Liebig et al., 2010; Schrier-Uijl et al., 2010; Hartmann et al., 2011). Furthermore, at the intensively managed site (CHA), LAI had comparable explanatory power as SWC. As mentioned above, step-changes in LAI during the growing period reflect management activities (fertilizer application at low LAI). Although ammonium-based fertilizers can inhibit CH_4 uptake (oxidation) by methanotrophs (Willison et al., 1995; Stiehl-Braun et al., 2011), SWC still had a highly significant impact on CH_4 fluxes at LAI < 1 (Fig. 8), indicating dominant environmental drivers.

4.1.3 CO_2 fluxes

Opaque soil chambers were used to exclusively measure respiratory fluxes, which were in the expected range from close to zero in winter up to 15 µmol m^{-2} s^{-1} during summer, similar to, e.g. Myklebust et al. (2008). Our chamber measurements did agree with eddy covariance-based respiration data, which were running simultaneously at all three sites (data not shown). Summer grazing at AWS did not have a big effect on temporal variability and magnitude of respiration, similar to findings by Lin et al. (2011).

BGD
10, 2635–2673, 2013

4.2 Diel variation of N_2O and CH_4 fluxes

In contrast to what we learned on the annual scale , highest emissions of N_2O of all three grasslands were observed at AWS, being twice the observed seasonal mean. As manure was applied to AWS pastures ten days prior to sampling, we likely captured a hot moment supporting our conclusion that management impacts are dominating N_2O flux variability. Already studies like Christensen (1983) and Flechard et al. (2007) already showed that peak emissions of N_2O appeared lagged to manure application (eight to 12 days).

In the literature, there is no consistent picture regarding the presence of significant diel patterns of N_2O and CH_4 fluxes (Christensen, 1983; Skiba et al., 1996; Maljanen et al., 2002; Duan et al., 2005; Hendriks et al., 2008; Baldocchi et al., 2012). Duan et al. (2005) suggested that the type of ecosystem might have an influence on the presence of diel N_2O and CH_4 flux variations. However, our study exclusively investigated grasslands and we found significant diel variations of N_2O fluxes for one out of three sites (FRU). These fluxes did correlate with air temperature, similar to the annual scale (Table 2). At CHA, changes in air temperature did affect N_2O fluxes less strongly, thus no significant diel patterns in N_2O fluxes were observed. This might be attributable to the fact that the last fertilizer application at CHA was more than three weeks prior to the intensive campaign, while FRU, in contrast, was grazed a few days before. Moreover, the vegetation composition at FRU exhibits a larger fraction of legumes. This suggests that not only ecosystem type, but also site specifics (e.g. management intensity or vegetation composition) might influence diel variations in N_2O fluxes.

In contrast to what we observed on the annual scale (Table 2), CH_4 fluxes were not constrained by changes in SWC over the course of 48 h, probably because changes were too small (decrease of less than 2 % vol.) to significantly affect the magnitude of CH_4 fluxes.

BGD
10, 2635–2673, 2013

4.3 Spatial patterns and auto-correlation

Working with soil chambers requires information on the spatial distribution of GHG fluxes at ecosystem scale to design appropriate experiments and to be able to correct mean ecosystem fluxes for potential biases. In relation to the magnitude of mean chamber fluxes of N_2O and CH_4, individual chamber fluxes are highly variable in space (e.g. Matthias et al., 1980; Folorunso and Rolston, 1984; Mosier et al., 1991), as they are largely determined by small-scale biochemical processes (Ambus and Christensen, 1994; Dalal and Allen, 2008).

We observed that out of our three sites, merely AWS exhibited permanent spots where CH_4 uptake was significantly smaller than at the rest of the transect. This corresponded well with local microtopographical conditions, i.e. the inclination of the terrain (Fig. 9). Chambers placed in terrain with greater inclination systematically exhibited lower SWC values. This in turn corresponded well with what was observed at the annual scale, where lower CH_4 uptake rates correlated significantly with higher SWC. At CHA and FRU, we observed that flux magnitudes varied spatially, hot spots were however not permanent. Thus, the situation at CHA and FRU represents the ideal case when trying to sample a representative mean of an ecosystem. Omitting permanent hot spots may lead to a systematic bias in GHG flux budgets. In our case, omitting chambers one to four at AWS would have lead to an underestimation of annual CH_4 uptake of roughly 5 % and an overestimation of annual N_2O emissions of 56 % (both, regarding annual budgets).

5 Conclusions

Highest mean annual emissions of N_2O were observed at the intensively managed site, whereas highest uptake rates of CH_4 were measured at the extensively managed site. This clearly illustrates the impact that management intensity has on the magnitude of N_2O and CH_4 fluxes in grasslands.

BGD
10, 2635–2673, 2013

We identified the known set of drivers for fluxes of CO_2, CH_4, and N_2O fluxes (T_a and SWC, for N_2O and CH_4, respectively). On the diel scale, T_a was found to a good predictor for N_2O fluxes at one site (FRU). At the intensively managed site (CHA), LAI proved to be a good proxy for management influence on fluxes of all three GHGs.

Spatial variability, especially of CH_4 and N_2O fluxes was high as expected. Permanent spots with lower CH_4 uptake, coincided with smaller inclination of the terrain on which chambers were placed. Thus, on sloping terrain, mean chamber fluxes of CH_4 should be estimated from an ensemble that is (a) big enough, and that (b) represents the average slope of the site. This is important as SWC is the major environmental driver.

Acknowledgements. We acknowledge the help of all Grassland Sciences Group Members from ETH Zurich who participated in the intensive observation campaign. We also thank our technicians Peter Pluess and Thomas Baur for station maintenance and technical support. This study was partially funded by the European Union Seventh Framework Program (FP7/2007–2013) under grant agreement no. 244122 (GHG-Europe). This study was further supported by COST Action ES0804. Advancing the integrated monitoring of trace gas exchange Between Biosphere and Atmosphere (ABBA).

References

Ambus, P. and Christensen, S.: Measurement of N_2O emission from a fertilized grassland: An analysis of spatial variability, J. Geophys. Res., 99, 16549–16555, 1994. 2638, 2654

Baldocchi, D., Detto, M., Sonnentag, O., Verfaillie, J., Teh, Y., Silver, W., and Kelly, N.: The challenges of measuring methane fluxes and concentrations over a peatland pasture, Agr. Forest Meteorol., 153, 177–187, doi:101016/jagrformet201104013, 2012. 2638, 2653

Ball, B., Horgan, G., Clayton, H., and Parker, J.: Spatial variability of nitrous oxide fluxes and controlling soil and topographic properties, J. Environ. Qual., 26, 1399–1409, 1997. 2638

Beniston, M.: Mountain climates and climatic change: An overview of processes focusing on the European Alps, Pure. Appl. Geophys., 162, 1587–1606, doi:10.1007/s00024-005-2684-9, 2005. 2637

BGD
10, 2635–2673, 2013

Boesch, H.: Nomadismus, Transhumanz und Alpwirtschaft, Die Alpen, 27, 202–207, 1951. 2638
Buchmann, N.: Greenhouse gas emissions from European grasslands and mitigation options, in: Grassland productivity and ecosystem services, edited by: LeMaire, G., Hodgson, J., and Chabbi, A., Grassland productivity and ecosystem services, CAB International, UK, 92–100, 2011. 2638
Chevan, A. and Sutherland, M.: Hierarchical partitioning, Amer. Statistician., 45, 90–96, 1991. 2643
Christensen, S.: Nitrious oxide emission from a soil under permanent grass: Seasonal and diurnal fluctuations as influenced by manuring and fertilization, Soil Biol. Biochem., 15, 531–536, 1983. 2653
Ciais, P., Soussana, J., Vuichard, N., Luyssaert, S., Don, A., Janssens, I., Piao, S., Dechow, R., Lathière, J., Maignan, F., Wattenbach, M., Smith, P., Ammann, C., Freibauer, A., Schulze, E., and CARBOEUROPE Synthesis Team: The greenhouse gas balance of European grasslands, Biogeosciences Discuss., 7, 5997–6050, doi:10.5194/bgd-7-5997-2010, 2010a. 2637
Ciais, P., Wattenbach, M., Vuichard, N., Smith, P., Piao, L., Don, A., Luyssaert, S., Janssens, I., Bondeau, A., Dechow, R., Leip, A., Smith, P., Beer, C., van der Werf, G., Gervois, S., van Oost, K., Tomelleri, E., Freibauer, A., and Schulze, E.: The European carbon balance, Part 2: Croplands, Glob. Change Biol., 16, 1409–1428, 2010b. 2637
Dalal, R. and Allen, D.: Greenhouse gas fluxes from natural ecosystems, Aust. J. Bot., 56, 369–407, 2008. 2638, 2654
Dietrich, C. and Osborne, M.: Estimation of covariance parameters in kriging via restricted maximum likelihood, Math. Geol., 23, 119–135, 1991. 2643
Duan, X., Wang, X., Mu, Y., and Ouyang, Z.: Seasonal and diurnal variations in methane emissions from Wuliangsu Lake in arid regions of China, Atmos. Environ., 39, 4479–4487, 2005. 2653
Efron, B.: Bootstrap methods: Another look at the jackknife, Ann. Stat., 7, 1–26, 1979. 2643
Ehlers, E. and Kreutzmann, H.: High mountain pastoralism in Northern Pakistan, Franz Steiner Verlag, Stuttgart, 2000. 2638, 2639
Finger, R., Gilgen, A., Prechsl, U., and Buchmann, N.: An economic assessment of drought effects on three grassland systems in Switzerland, Reg. Environ. Change, doi:10.1007/s10113-012-0346-x, 2012. 2639

BGD
10, 2635–2673, 2013

Flechard, C., Ambus, P., Skiba, U., Rees, R., Hensen, A., van Amstel, A., van den Pol-van Dasselaar, A., Soussana, J., Jones, M., Clifton-Brown, J., Raschi, A., Horvath, L., Neftel, A., Jocher, M., Ammann, C., Leifeld, J., Fuhrer, J., Calanca, P., Thalman, E., Pilegaard, K., Marco, C. D., Campbell, C., Nemitz, E., Hargreaves, K., Levy, P., Ball, B., Jones, S., van de Bulk, W., Groot, T., Blom, M., Domingues, R., Kasper, G., Allard, V., Ceschia, E., Cellier, P., Laville, P., Henault, C., Bizouard, F., Abdalla, M., Williams, M., Baronti, S., Berretti, F., and Grosz, B.: Effects of climate and management intensity on nitrous oxide emissions in grassland systems across Europe, Agr. Ecosyst. Environ., 121, 135–152, 2007. 2653

Flessa, H., Ruser, R., Schilling, R., Loftfield, N., Munch, J., Kaiser, E., and Beese, F.: N_2O and CH_4 fluxes in potato fields: Automated measurement, management effects and temporal variation, Geoderma, 105, 307–325, 2002. 2637, 2638

Folorunso, O. and Rolston, D.: Spatial variability of field-measured denitrification gas fluxes, Soil Sci. Soc. Am. J., 48, 1214–1219, 1984. 2638, 2651, 2654

Glatzel, S. and Stahr, K.: Methane and nitrous oxide exchange in differently fertilised grassland in southern Germany, Plant Soil, 231, 21–35, 2001. 2651

Hartmann, A., Buchmann, N., and Niklaus, P.: A study of soil methane sink regulation in two grasslands exposed to drought and N fertilization, Plant Soil, 342, 265–275, 2011. 2640, 2641, 2652

Hendriks, D., Dolman, A., Van der Molen, J., and van Huissteden, J.: A compact and stable eddy covariance set-up for methane measurements using off-axis integrated cavity output spectroscopy, Atmos. Chem. Phys., 8, 431–443, doi:10.5194/acp-8-431-2008, 2008. 2653

IPCC, W.: The physical science basis. Contribution of working group I to the fourth assessment report of the Intergovernmental Panel on Climate Change, in: Climate Change 2007, edited by: Solomon, S., Qin, D., Manning, M., Chen, Z., Marquis, M., Averyt, K., Tignor, M., and Miller, H., Cambridge University Press, Cambridge, 210–215, 2007. 2637

Janssens, I., Freibauer, A., Ciais, P., Smith, P., Nabuurs, G., Folberth, G., Schlamadinger, B., Huties, R., Ceulemans, R., Schulze, E., Valentini, R., and Dolman, A.: Europe's terrestrial biosphere absorbs 7 to 12 % of European anthropogenic CO_2 emissions, Science, 300, 1538–1542, 2003. 2637

Jiang, C., Yu, G., Fang, H., Cao, G., and Li, Y.: Short-term effect of increasing nitrogen deposition on CO_2, CH_4 and N_2O fluxes in an alpine meadow on the Qinghai-Tibetan Plateau, China, Atmos. Environ., 44, 2920–2926, 2010. 2638

BGD
10, 2635–2673, 2013

Jones, S., Rees, R., Kosmas, D., Ball, B., and Skiba, U.: Carbon sequestration in a temperate grassland; management and climate controls, Soil Use Manage., 22, 132–142, 2006. 2638
Lessard, R., Rochette, P., Gregorich, E., Desjardins, R., and Pattey, E.: CH_4 fluxes from a soil amended with dairy cattle manure and ammonium nitrate, Can. J. Soil Sci., 77, 179–186, 1997. 2652
Liebig, M., Gross, J., Kronberg, S., Phillips, R., and Hanson, J.: Grazing management contributions to net global warming potential: A long-term evaluation in the northern Great Plains, J. Environ. Qual., 39, 799–809, 2010. 2651, 2652
Lin, X., Zhang, Z., Wang, S., Hu, Y., Xu, G., Luo, C., Chang, X., Duan, J., Lin, Q., Xu, B., Wang, Y., Zhao, X., and Xie, Z.: Response of ecosystem respiration to warming and grazing during the growing seasons in the alpine meadow on the Tibetan plateau, Agr. Forest Meteorol., 151, 792–802, 2011. 2652
Maljanen, M., Martikainen, P., Aaltonen, H., and Silvola, J.: Short-term variation in fluxes of carbon dioxide, nitrous oxide and methane in cultivated and forested organic boreal soils, Soil Biol. Biochem., 34, 577–584, 2002. 2653
Mathieu, O., Leveque, J., Heault, C., Milloux, M., Bizouard, F., and Andreux, F.: Emissions and spatial variability of N_2O, N_2 and nitrous oxide mole fraction at the field scale, Soil Biol. Biochem., 38, 941–951, 2006. 2638
Matthias, A., Blackmer, A., and Bremner, J.: A simple chamber technique for field measurement of emissions of nitrous oxide from soils, J. Environ. Qual., 9, 251–256, 1980. 2638, 2654
Merbold, L., Ziegler, W., Mukelabai, M., and Kutsch, W.: Spatial and temporal variation of CO_2 efflux along a disturbance gradient in a miombo woodland in Western Zambia, Biogeosciences, 8, 147–164, doi:10.5194/bg-8-147-2011, 2011. 2638
Michna, P., Eugster, W., Hiller, R., Zeeman, M., and Wanner, H.: Topoclimatological case-study of Alpine pastures near the Albula pass in the Eastern Swiss Alps, Geograph Helv, in revision, 2013. 2639
Mosier, A., Schimel, D., Valentine, D., Bronson, K., and Parton, W.: Methane and nitrous oxide fluxes in native, fertilized and cultivated grasslands, Nature, 350, 330–332, 1991. 2651, 2654
Mosier, A., Delgado, J., Cochran, V., Valentine, D., and Parton, W.: Impact of agriculture on soil consumption of atmospheric CH_4 and a comparison of CH_4 and N_2O flux in subartic, temperate and tropical grasslands, Nutr. Cycl. Agroecosys., 49, 71–83, 1997. 2652

BGD
10, 2635–2673, 2013

Myklebust, M., Hipps, L., and Ryel, R.: Comparison of eddy covariance, chamber, and gradient methods of measuring soil CO_2 efflux in an annual semi-arid grass, *Bromus tectorum*, Agr. Forest Meteorol., 148, 1894–1907, 2008. 2652

Neftel, A., Flechard, C., Ammann, C., Conen, F., Emmenegger, L., and Zeyer, K.: Experimental assessment of N_2O background fluxes in grassland systems, Tellus B, 59, 470–482, 2007. 2651

Pumpanen, J., Kolari, P., Ilvesniemi, H., Minkkinen, K., Vesala, T., Niinistö, S., Lohila, A., Larmola, T., Morero, M., Pihlatie, M., Janssens, I., Yuste, J., Gruenzweig, J., Reth, S., Subke, J., Savage, K., Kutsch, W., Ostreng, G., Ziegler, W., Anthoni, P., and Hari, P.: Comparison of different chamber techniques for measuring soil CO_2 efflux, Agr. Forest Meteorol., 123, 159–176, 2004. 2637

R Development Core Team: R: A Language and Environment for Statistical Computing, R Foundation for Statistical Computing, Vienna, Austria, http://www.R-project.org, ISBN 3-900051-07-0, 2010. 2641

Ribeiro, P. and Diggle, P.: geoR: A package for geostatistical analysis, R-NEWS, 1, 15–18, 2001. 2643

Rochette, R.: Towards a standard non-steady-state chamber methodology for measuring soil N_2O emissions, Anim. Feed Sci. Tech., 166–167, 141–146, 2011. 2638

Ryden, J.: N_2O exchange between a grassland soil and the atmosphere, Nature, 292, 235–237, 1981. 2651

Schaufler, G., Kitzler, B., Schindlbacher, A., Skiba, U., Sutton, M., and Zechmeister-Boltenstern, S.: Greenhouse gas emissions from European soils under different land use: effects of soil moisture and temperature, Eur. J. Soil Sci., 61, 683–696, 2010. 2651

Schrier-Uijl, A., Kroon, P., Hensen, A., Leffelaar, P., Berendse, F., and Veenendaal, E.: Comparison of chamber and eddy covariance-based CO_2 and CH_4 emission estimates in a heterogeneous grass ecosystem on peat, Agr. Forest Meteorol., 150, 825–831, 2010. 2652

Schulze, E., Luyssaert, S., Ciais, P., Freibauer, A., Janssens, I., Soussana, J., Smith, P., Grace, J., Levin, I., Thiruchittampalam, B., Heimann, M., Dolman, A., Valentini, R., Bousquet, P., Peylin, P., Peters, W., Rodenbeck, C., Etiope, G., Vuichard, N., Wattenbach, M., Nabuurs, G., Poussi, Z., Nieschulze, J., and Gash, J.: Importance of methane and nitrous oxide for Europe's terrestrial greenhouse-gas balance, Nat. Geosci., 2, 842–850, 2009. 2637

Scott, A., Crichton, I., and Ball, B.: Long-term monitoring of soil gas fluxes with closed chambers using automated and manual systems, J. Environ. Qual., 28, 1637–1643, 1999. 2641

BGD
10, 2635–2673, 2013

Sieber, R., Hollenstein, L., Odden, B., and Hurni, L.: From classic atlas design to collaborative platforms – The SwissAtlasPlatform Project, in: Proceedings of the 25th international conference of the ICA, Paris, France, 2011. 2639

Skiba, U., Hargreaves, K., Beverland, I., O'Neil, D., Fowler, D., and Moncrieff, J.: Measurement of field scale N_2O emission fluxes from a wheat crop using micrometeorological techniques, Plant Soil, 181, 139–144, 1996. 2653

Soussana, J., Allard, V., Pilegaard, K., Ambus, P., Ammann, C., Campbell, C., Ceschia, E., Clifton-Brown, J., Czobel, S., Domingues, R., Flechard, C., Fuhrer, J., Hansen, A., Horvath, L., Jones, M., Kasper, G., Martin, C., Nagy, Z., Neftel, A., Raschi, A., Baronti, S., Rees, R., Skiba, U., Stefani, P., Manca, G., Sutton, M., Tuba, Z., and Valentini, R.: Full accounting of the greenhouse gas (CO_2, N_2O, CH_4 budget of nine European grassland sites, Agr. Ecosyst. Environ., 121, 121–134, 2007. 2637

Stiehl-Braun, P., Hartmann, A., Kandeler, E., Buchmann, N., and Niklaus, P.: Interactive effects of drought and N fertilization on the spatial distribution of methane assimilation in grassland soils, Glob. Change Biol., 17, 2629–2639, 2011. 2652

Stone, M.: Cross-validatory choice and assessment of statistical predictions, J. R. Stat. Soc., 36, 111–147, 1974. 2643

van den Pol-van Dasselaar, A., Corre, W., Prieme, A., Klemedtsson, A., Weslien, P., Stein, A., Klemedtsson, L., and Oenema, O.: Spatial variability of methane, nitrous oxide, and carbon dioxide emissions from drained grasslands, Soil Sci. Soc. Am. J., 62, 810–817, 1998. 2638

Velthof, G., van Groeningen, J., Gebauer, G., Pietrzak, S., Jarvis, S., Pinto, M., Corre, W., and Oenema, O.: Temporal stability of spatial patterns of nitrous oxide fluxes from sloping grassland, J. Environ. Qual., 29, 1297–1407, 2000. 2651

Vleeshouwers, L. and Verhagen, A.: Carbon emission and sequestration by agricultural land use: a model study for Europe, Glob. Change Biol., 8, 519–530, 2002. 2637

Wagner-Riddle, C., Thurtell, G., Kidd, G., Beauchamp, E., and Sweetman, R.: Estimates of nitrous oxide emissions from agricultural fields over 28 months, Can. J. Soil Sci., 77, 135–144, 1997. 2651

Wang, Y., Xue, M., Zheng, X., Ji, B., Du, R., and Wang, Y.: Effects of environmental factors on N_2O emission from and CH_4 uptake by the typical grasslands in the Inner Mongolia, Chemosphere, 58, 205–215, 2005. 2637, 2651

Weiss, R.: Das Alpwesen Graubündens: Wirtschaft, Sachkultur, Recht, Älplerarbeit und Älplerleben, Eugen Rentsch Verlag, Erlenbach–Zürich, 1941. 2638

BGD
10, 2635–2673, 2013

Willison, T., Webster, C., Goulding, K., and Powlson, D.: Methane oxidation in temperate soils – effects of land-use and the chemical form of the nitrogen fertilizer, Chemsophere, 30, 539–546, 1995. 2652

Zeeman, M., Hiller, R., Gilgen, A., Michna, P., Pluess, P., Buchmann, N., and Eugster, W.: Management and climate impacts on the net CO_2 fluxes and carbon budgets of three grasslands along an elevational gradient in Switzerland, Agr. Forest Meteorol., 150, 519–530, 2010. 2640, 2664

BGD

10, 2635–2673, 2013

Table 1. Model performance of maximum likelihood (ML), restricted maximum likelihood (RML), ordinary least squares (OLS) and weighted least squares (WLS) fits for annually averaged chamber fluxes at Alp Weissenstein; r^2 values (model on observation) and p-values are given.

	ML	RML	OLS	WLS
N_2O				
r^2	0.4	0.4	0.19	0.16
p-value	0.005	0.005	0.05	0.06
CH_4				
r^2	0.4	0.39	0.33	0.29
p-value	0.005	0.006	0.01	0.02
CO_2				
r^2	0.18	0.21	0.25	0.22
p-value	0.05	0.04	0.03	0.04

BGD
10, 2635–2673, 2013

Table 2. Multiple linear regression models for annual greenhouse gas fluxes at all three sites (CHA = Chamau; FRU = Fruebuel; AWS = Alp Weissenstein). For the overall model performance, p-values and adjusted r^2 (in brackets) are given. For the individual drivers (T_a = air temperature; SWC = soil water content; LAI = leaf area index), only p-values are given.

	CHA	FRU	AWS
N_2O	p (adj. r^2)	p (adj. r^2)	p (adj. r^2)
overall	0.002 (0.42)	0.211 (0.19)	0.227 (0.34)
T_a	0.002	0.042	0.925
SWC	0.126	0.269	0.164
LAI	0.002	0.982	0.210
CH_4			
overall	0.003 (0.41)	0.002 (0.51)	< 0.001 (0.83)
T_a	0.744	0.471	0.749
SWC	0.025	< 0.001	< 0.001
LAI	0.01	0.616	0.061
CO_2			
overall	< 0.001 (0.8)	< 0.001 (0.8)	0.084 (0.47)
T_a	< 0.001	< 0.001	0.106
SWC	0.013	0.71	0.196
LAI	0.005	0.11	0.424

BGD
10, 2635–2673, 2013

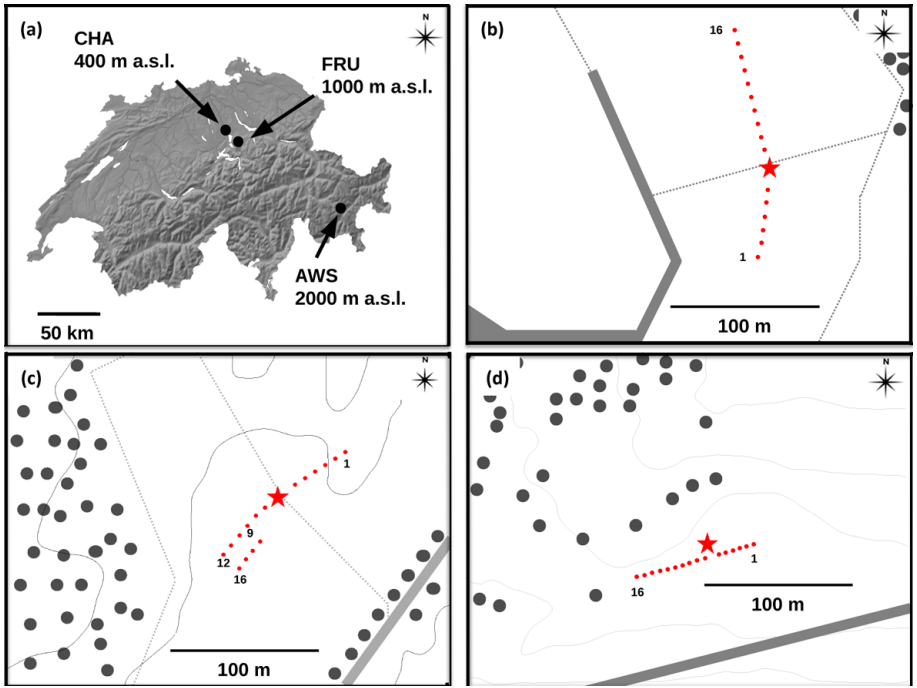

Fig. 1. Topographical map of Switzerland **(a)** showing the geographic position of the sites, **(b)** Chamau (CHA), **(c)** Fruebuel (FRU), and **(d)** Alp Weissenstein (AWS) as well as site set-up maps **(b–d)**. The red star indicates the position of the eddy covariance tower and the red dots the position of the chambers along the prevailing wind direction (flux footprint; see Zeeman et al., 2010, for details). The numbers refer to the chamber numbers along the transects. Dots denote individual trees and gray bold lines paved roads.

BGD
10, 2635–2673, 2013

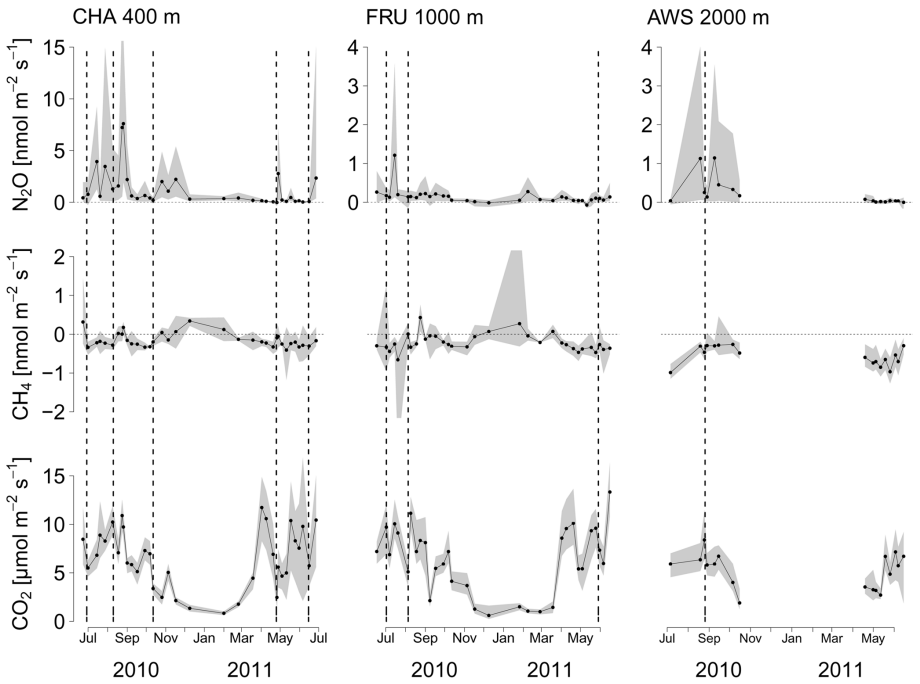

Fig. 2. Annual courses of N_2O, CH_4 and CO_2 fluxes at Chamau (CHA), Fruebuel (FRU) and Alp Weissenstein (AWS). The black lines indicate the mean ecosystem flux of the respective greenhouse gas and the gray shaded areas indicate the 95 % confidence intervals. Dashed, vertical lines indicate fertilizer applications. Note the different scaling for N_2O fluxes at the three sites. Fluxes of N_2O and CH_4 are given in nmol m^{-2} s^{-1} and CO_2 in µmol m^{-2} s^{-1}.

BGD
10, 2635–2673, 2013

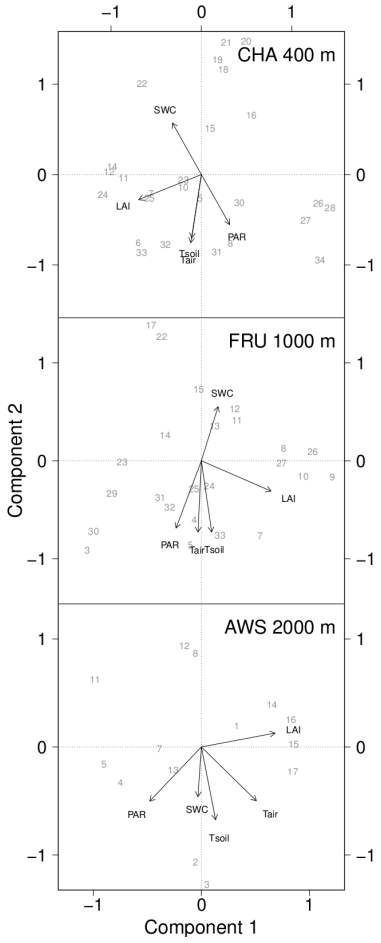

Fig. 3. Caption on next page.

BGD
10, 2635–2673, 2013

Fig. 3. Biplots of the first two components of a standardized principal component analysis of environmental variables for the three sites, Chamau (CHA), Fruebuel (FRU), and Alp Weissenstein (AWS). Environmental variables measured during sampling campaigns within the 12-month study period were considered (numbers 1 to 34). T_a = air temperature; T_s = soil temperature; SWC = soil water content; LAI = leaf area index; PAR = photosynthetic active radiation.

BGD
10, 2635–2673, 2013

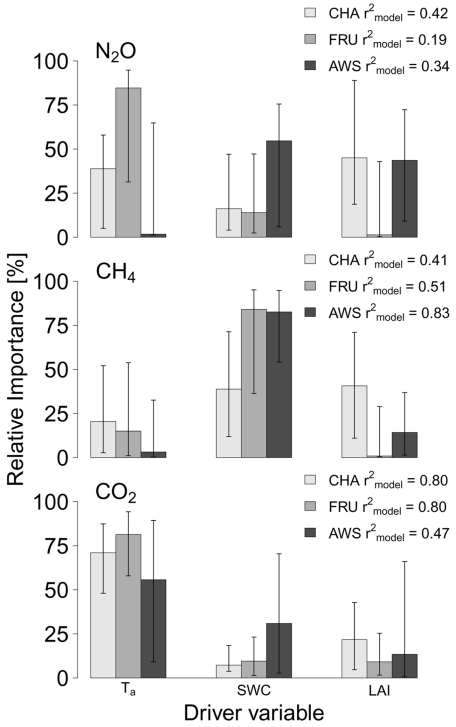

Fig. 4. Explanatory power of driver variables for greenhouse gas fluxes on the annual time scale, with T_a as air temperature, SWC as soil water content, and LAI as leaf area index. Contribution (relative importance) to the overall variance explained is given in %. Error bars indicate 95 % confidence intervals as determined from bootstrapping (N_{runs} = 1000). r^2 values represent overall model performance. Significance levels of each driver can be found in Table 2. The upper panel shows the model performance at all three sites for N_2O fluxes, the mid panel for CH_4 fluxes, and the lower panel for CO_2 fluxes. CHA = Chamau; FRU = Fruebuel; AWS = Alp Weissenstein.

BGD
10, 2635–2673, 2013

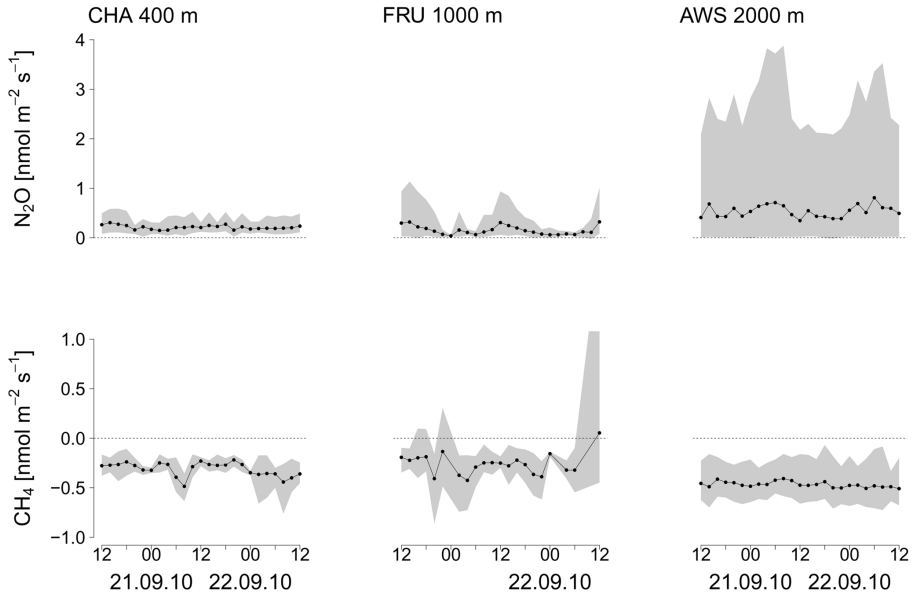

Fig. 5. Diel courses of N_2O (top) and CH_4 (bottom) fluxes at CHA = Chamau, FRU = Fruebuel, and AWS = Alp Weissenstein. The gray shaded areas indicate the 95 % confidence intervals of mean chamber fluxes (black line).

BGD
10, 2635–2673, 2013

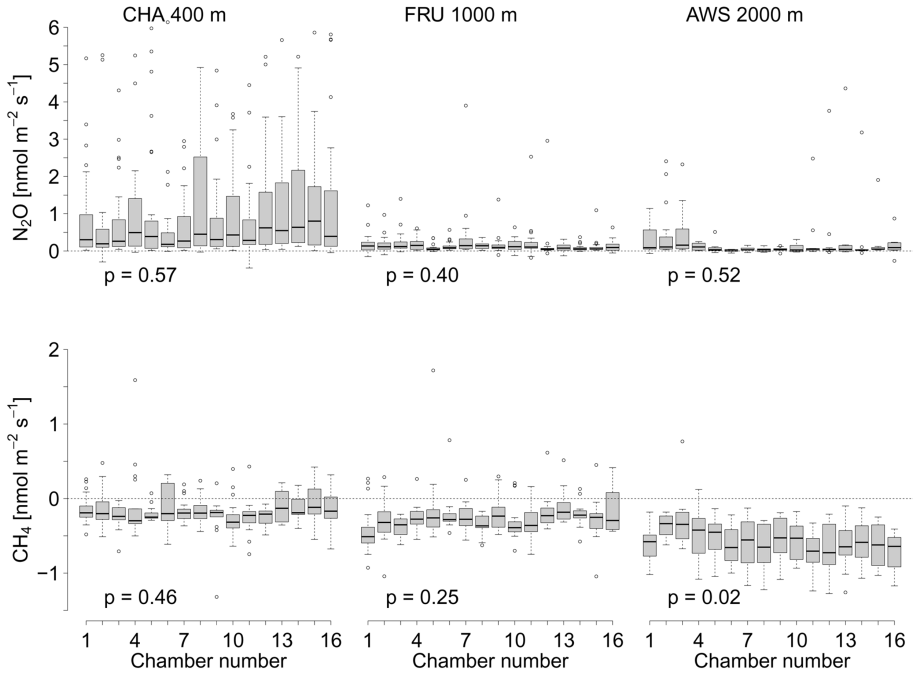

Fig. 6. Boxplots depicting spatial gradients of mean annual N_2O and CH_4 chamber fluxes (1–16 on x-axis) at Chamau (CHA), Fruebuel (FRU), and Alp Weissenstein (AWS). The p-values refer to the ANOVA results with chamber as factor. Values below 0.05 indicate significant differences among mean chamber fluxes over the 12-month study period.

BGD
10, 2635–2673, 2013

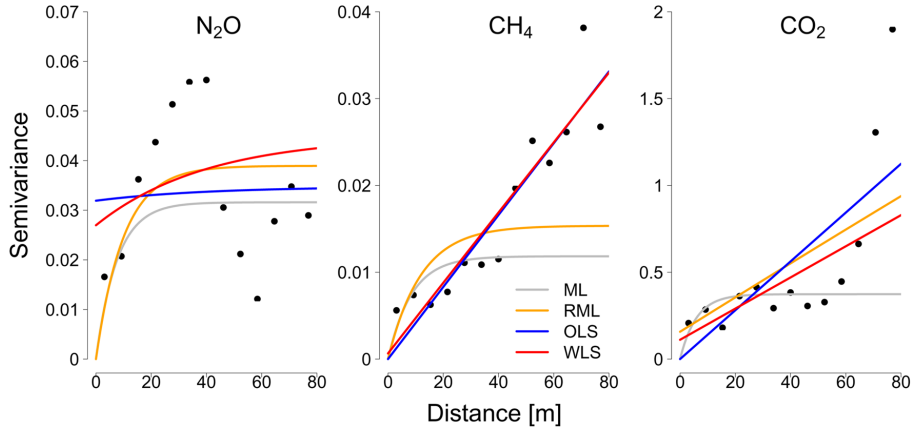

Fig. 7. Empirical and modeled variogramms (black points) for Alp Weissenstein for annually averaged N_2O, CH_4 and CO_2 chamber fluxes. For N_2O and CH_4 fluxes, semivariance is given in nmol m^{-2} s^{-1} and for CO_2 in µmol m^{-2} s^{-1}. Fitted models are (1) ML = maximum likelihood, (2) RML = restricted maximum likelihood, (3) OLS = ordinary least squares, and (4) WLS = weighted least squares.

BGD
10, 2635–2673, 2013

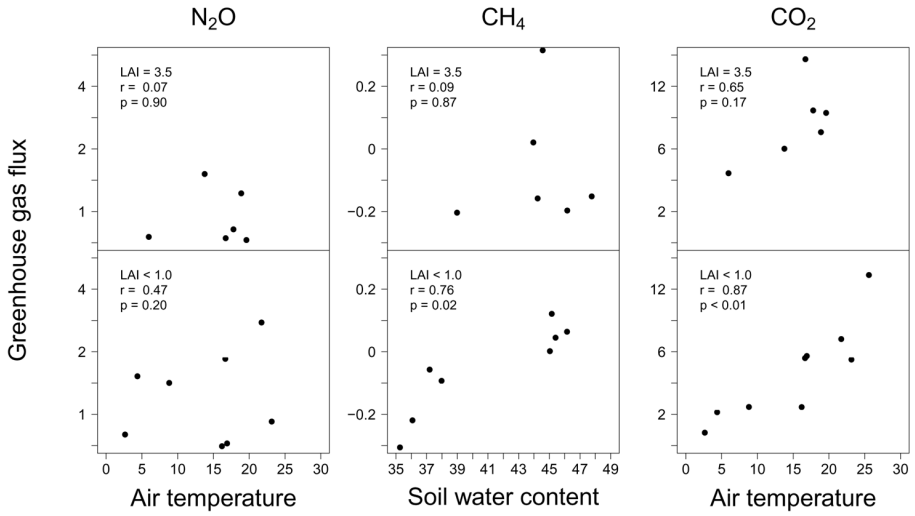

Fig. 8. Relationships of mean chamber greenhouse gas fluxes and their primary environmental drivers at two different LAI for the intensively managed site Chamau. For CH_4 and N_2O, fluxes are given in nmol m^{-2} s^{-1}, for CO_2 in µmol m^{-2} s^{-1}. Soil water content is given in vol. %, and air temperature in °C. Correlation coefficients and p-values are given.

BGD
10, 2635–2673, 2013

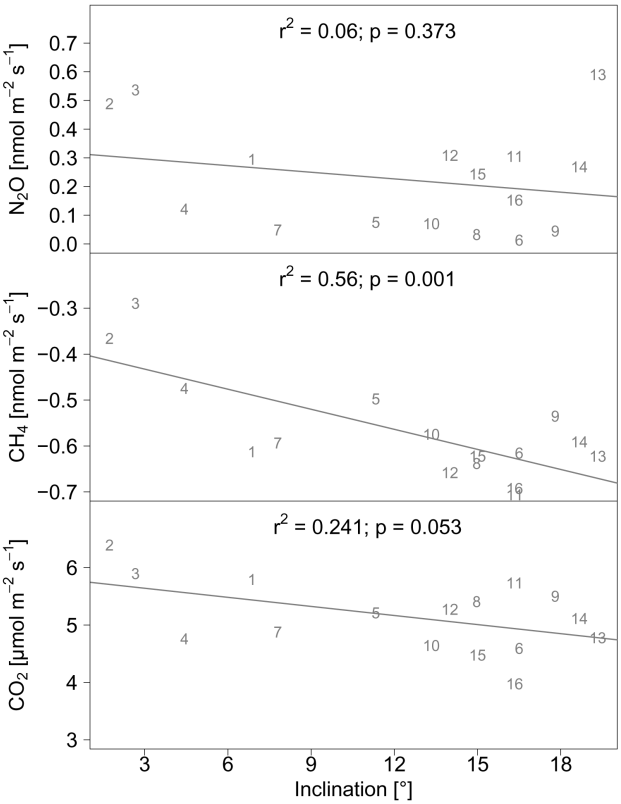

Fig. 9. Annually averaged chamber fluxes of N_2O, CH_4, and CO_2 at Alp Weissenstein plotted against inclination at the respective chambers. The numbers indicate the chamber position along the transect. Regression coefficients as well as p-values are given.

BGD
10, 2635–2673, 2013